JPIS
Journal of Periodontal & Implant Science

Research Article

Check for updates

Biomimetic characteristics of mussel adhesive protein-loaded collagen membrane in guided bone regeneration of rabbit calvarial defects

Woong-Kyu Song [iD] [1], **Joo-Hyun Kang** [iD] [1], **Jae-Kook Cha** [iD] [1], **Jung-Seok Lee** [iD] [1], **Jeong-Won Paik** [iD] [1], **Ui-Won Jung** [iD] [1], **Byung-Hoon Kim** [iD] [2], **Seong-Ho Choi** [iD] [1,*]

[1]Department of Periodontology, Research Institute for Periodontal Regeneration, Yonsei University College of Dentistry, Seoul, Korea
[2]Department of Dental Materials, Chosun University School of Dentistry, Gwangju, Korea

[lock] OPEN ACCESS

*Correspondence:
Seong-Ho Choi
Department of Periodontology, Research Institute for Periodontal Regeneration, Yonsei University College of Dentistry, 50-1 Yonsei-ro Seodaemun-gu, Seoul 03722, Korea.
E-mail: shchoi726@yuhs.ac
Tel: +82-2-2228-3189
Fax: +82-2-392-0398

ORCID iDs
Woong-Kyu Song [iD]
https://orcid.org/0000-0002-6365-5544
Joo-Hyun Kang [iD]
https://orcid.org/0000-0001-5444-5791
Jae-Kook Cha [iD]
https://orcid.org/0000-0002-6906-7209
Jung-Seok Lee [iD]
https://orcid.org/0000-0003-1276-5978
Jeong-Won Paik [iD]
https://orcid.org/0000-0002-5554-8503
Ui-Won Jung [iD]
https://orcid.org/0000-0001-6371-4172
Byung-Hoon Kim [iD]
https://orcid.org/0000-0002-5008-1465
Seong-Ho Choi [iD]
https://orcid.org/0000-0001-6704-6124

ABSTRACT

Purpose: The aim of the present study was to evaluate the biocompatibility and barrier function of mussel adhesive protein (MAP)-loaded collagen membranes in guided bone regeneration (GBR).

Methods: Eight male New Zealand white rabbits were used. Four circular defects (diameter: 8 mm) were created in the calvarium of each animal. The defects were randomly assigned to 1) a negative control group, 2) a cyanoacrylate (CA)-loaded collagen membrane group (the CA group), 3) a MAP-loaded collagen membrane group (the MAP group), and 4) a group that received a polycaprolactone block with MAP-loaded collagen membrane (the MAP-PCL group). Specimens were harvested at 2 weeks (n=4) and 8 weeks (n=4) postoperatively for observational histology and histometric analysis.

Results: In the histologic analysis, MAP was completely absorbed without any byproducts. In contrast, some of the CA adhesive remained, showing an inflammatory reaction, at 8 weeks. In the MAP-PCL group, the MAP-loaded collagen membranes served as a barrier membrane despite their fast degradation in GBR. No significant difference was found in the amount of new bone between the MAP-PCL and MAP groups (1.82±0.86 mm^2 and 2.60±0.65 mm^2, respectively).

Conclusions: The MAP-loaded collagen membrane functioned efficiently in this rabbit calvarial GBR model, with excellent biocompatibility. Further research is needed to assess clinical applications in defect types that are more challenging for GBR than those used in the current model.

Keywords: Bone regeneration; *Mytilus edulis*; Polymers; Tissue adhesives

INTRODUCTION

Guided bone regeneration (GBR) is a well-established procedure for augmentation of a deficient alveolar ridge to place an implant [1]. For GBR to be successful, various factors, including space stability and graft consolidation, need to be considered [2]. Several methods,

Author Contributions
Conceptualization: Woong-Kyu Song, Ui-Won Jung, Seong-Ho Choi; Data Curation: Woong-Kyu Song; Formal analysis: Woong-Kyu Song, Joo-Hyun Kang, Seong-Ho Choi; Funding Acquisition: Seong-Ho Choi; Investigation: Woong-Kyu Song, Jae-Kook Cha, Jeong-Won Paik, Seong-Ho Choi; Methodology: Woong-Kyu Song, Jung-Seok Lee, Ui-Won Jung, Byung-Hoon Kim, Seong-Ho Choi; Project administration: Woong-Kyu Song; Resources: Byung-Hoon Kim, Seong-Ho Choi; Supervision: Seong-Ho Choi; Writing - original draft: Woong-Kyu Song, Joo-Hyun Kang, Jae-Kook Cha, Jeong-Won Paik, Seong-Ho Choi; Writing - review & editing: Woong-Kyu Song, Jae-Kook Cha, Jeong-Won Paik, Jung-Seok Lee, Ui-Won Jung, Byung-Hoon Kim, Seong-Ho Choi.

Conflict of Interest
No potential conflict of interest relevant to this article was reported.

such as suturing and screw or tag placement, have been suggested for the fixation of a membrane to maintain a secluded space and prevent the displacement of the graft. However, the use of these tools complicates the procedure, and an additional intervention is required to remove these materials [2]. Application of surgical adhesive appears to be a convenient method for membrane fixation, because of its fast application and the fact that it does not require removal [3]. In dentistry, cyanoacrylate (CA), as a representative surgical adhesive, has been widely used for decades to replace sutures, for membrane fixation, and to repair sinus membrane perforations [3-5]. However, some reports have shown that it is not fully absorbed, and its remnants may cause adverse reactions [6-8].

Mussel adhesive protein (MAP) from the *Mytilus* genus is secreted by the mussel foot, and has attracted significant attention for potential use in biomedical applications. This substance is composed of more than 8 different proteins responsible for coating and adhesion of the mussel byssus. MAP enables mussels to attach to rocks in marine environments, which are typically characterized by humidity, salinity, tides, and waves [9]. In addition, it allows adhesion to various substrates, including metal, glass, plastic, and living body substances [9-14]. MAP is rich in the amino acid tyrosine, which by enzymatic modification, is transformed to 3,4-dihydroxyphenyl-L-alanine (DOPA) [14]. Several studies have found the adhesive strength of MAP to be associated with its DOPA content [15-17].

During recent years, many research activities have been carried out to explore applications of this biomimetic adhesive protein in clinical settings, and several *in vitro* experiments have shown that MAP is a biocompatible and biodegradable material at the cellular level [18-21]. However, insufficient preclinical studies of MAP have been conducted.

Therefore, the purpose of the present study was to investigate the biocompatibility of MAP and the barrier function of MAP-loaded collagen membranes in GBR of the rabbit calvarium.

MATERIALS AND METHODS

Animals

Eight male New Zealand white rabbits (mean body weight, 2.8–3.2 kg; 8 weeks old) were included in this study. A power calculation was performed with new bone area (NB) as the primary outcome using a power analysis program (G*Power 3.1 software, University of Kiel, Kiel, Germany). Based upon the data of Sohn et al. [22], 8 subjects were suggested as a necessary sample size (assumed mean and standard deviation: 2 weeks, 1.88 ± 0.67 mm^2; 8 weeks, 3.19 ± 0.27 mm^2; power: 0.80; $\alpha < 0.05$).

All animals were managed in separate cages with standard laboratory conditions and provided with standard diets. All processes, including animal selection, management, preparation, and the surgical procedure, followed a protocol approved by the Institutional Animal Care and Use Committee, Yonsei Medical Center, Seoul, Korea (approval number 2017–0118).

Materials

A bilayer, chemically cross-linked collagen membrane (Rapigide, Dalim Tissen Co., Ltd., Seoul, Korea) was used as a carrier for MAP and CA. The membrane was derived from porcine skin and was composed of type I collagen.

MAP (ACRO Biosystems, Newark, DE, USA) was used as an adhesive for membrane fixation in this study. MAP adhesive is a formulation of the polyphenolic proteins extracted from the marine mussel, *Mytilus edulis*.

CA (Histoacryl, B. Braun Surgical SA, Barcelona, Spain) was used as a positive control for membrane fixation.

A 3-dimensional (3D) printed polycaprolactone (PCL) block (average molecular weight: 45,000 g/mol) was purchased from Polysciences, Inc. (Warrington, PA, USA) and scaffolds were prepared using a 3D printing machine (3D Bio Printer M4T-100, Mechatronics 4 Technology [M4T], Daegu, Korea). The PCL flakes were melted at 100°C in the heating cylinder and ejected through a heated nozzle of compressed air at a pressure of 300 kPa, with a feed rate of 50 mm/min. The scaffold struts could be plotted as a layer-by-layer deposition on a stage. The 3D scaffolds (strut size: 520–540 μm; pore size: 240–260 μm) were fabricated into discs (diameter: 8 mm; height: 1.9 mm).

Study design

Four circular defects measuring 8 mm in diameter were created in each rabbit calvarium [22]. The defects were then randomly assigned to the following 4 groups and filled with each material (Figure 1). The animals were sacrificed at either 2 weeks (n=4) or 8 weeks (n=4).

- Control group: The defect was filled with blood coagulum.
- CA group: The defect was covered by CA-loaded collagen membrane.
- MAP group: The defect was covered by MAP-loaded collagen membrane.
- MAP-PCL group: The defect was filled with a PCL block and covered by MAP-loaded collagen membrane.

Surgical protocol

General anesthesia was started using a subcutaneous injection of alfaxan (5 mg/kg) and maintained with inhalations of isoflurane (2%–2.5%). The head of the rabbit was shaved and disinfected using povidone iodine and alcohol before local anesthetic injections with
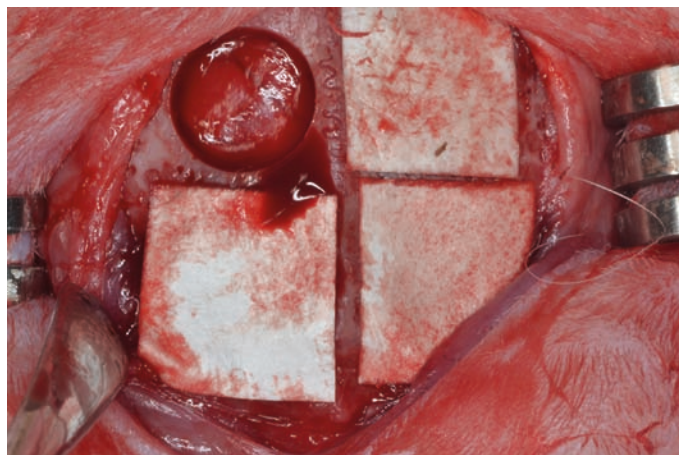
Figure 1. Four circular defects (diameter: 8 mm) were created in the calvarium of each rabbit, and were randomly assigned, moving clockwise from the top left: control group, CA group, MAP group, MAP-PCL group. Specimens were harvested at 2 and 8 weeks postoperatively.
CA: cyanoacrylate, MAP: mussel adhesive protein, MAP-PCL: mussel adhesive protein-polycaprolactone.

2% lidocaine. A sagittal incision was made along the midline of the cranium from the frontal bone to occipital bone and a full-thickness flap was elevated. Under copious saline irrigation, 4 circular osteotomies with a diameter of 8 mm were made using a trephine bur. In the MAP-PCL group, PCL blocks were implanted into the defect site, and a spinning movement was not observed. For groups using the barrier membrane, the membranes were cut to the size of 10×10 mm to cover each defect and the adhesive was applied on the side of the membrane facing the defect. The adhesive-loaded membranes were slightly sticky and fixed into the proper position. The flaps were then repositioned without tension and sutured with 4-0 absorbable suture material (Vicryl, Ethicon, Somerville, NJ, USA). The animals were sacrificed at either 2 weeks (n=4) or 8 weeks (n=4) postoperatively.

Clinical observations
Animals were carefully observed and evaluated for inflammation, allergic reactions, and other complications around the surgical site at 2 and 8 weeks after surgery.

Histological and histometric analysis
The fixed specimens were decalcified in 5% formic acid for 14 days and embedded in a paraffin block. Serial 5-μm-thick sections were cut through the central portion of each calvarial defect. Sections from each block were stained with hematoxylin and eosin and Masson trichrome for histologic and histometric analysis. The specimens were examined using a microscope (DM LB, Leica Microsystems, Wetzlar, Germany) equipped with a camera (DC300F, Leica Microsystems) by 1 blinded examiner. The slide images were saved as digital files, and computer-aided histometric measurements were performed using an image editing program (Adobe Photoshop CS6 version 13.0.1 ×32, Adobe Systems Inc, San Jose, CA, USA). For evaluating bone healing and regeneration, the following parameters were measured in each histologic section of the defect areas.

- Total augmented area (TA; mm^2): The area between the defect margins, including bony structures, residual materials, adipose tissue, and connective tissue. The superior boundary of the area is the collagen membrane or periosteum.
- NB (mm^2): Area of newly formed bone within the defect.
- Residual graft material area (RG; mm^2): Area of the remaining bone graft particles within the defect.
- %NB: Ratio of NB to TA.

Statistical analysis
The statistical analysis was conducted using commercially available software (SPSS 24.0, IBM Corp., Armonk, NY, USA). The descriptive data from histometric records were presented as mean values with the standard deviation. The Kruskal-Wallis test was used for comparisons among the 4 groups at each time point. Additionally, the Mann-Whitney U test was used to analyze differences between the 2 healing periods within the same experimental group. The statistical significance level was 5%.

RESULTS

Clinical observations
All the rabbits recovered without any problems, and the surgical sites healed without complications, such as severe swelling, infection, or exposure of the membrane or PCL block.

Histological analysis

Control group
At 2 weeks, the defects consisted of new bone and connective tissue with abundant blood vessels. Newly formed bone was observed from the defect margin to the center, and showed the appearance of woven bone. The central part of the defects was depressed and flattened by the overlying soft tissue and dura mater (Figures 2A and 3A).

At 8 weeks, a greater amount of new bone was found in the defect area than after 2 weeks of healing. In 1 of the 4 specimens, almost full closure along the outer surface of the defect was observed (Figures 4A and 5A).

CA group
At 2 weeks, the collagen membranes remained structurally intact and large empty spaces existed below them. The center of the defects had collapsed and bone regeneration was observed near the defect margin (Figures 2B and 3B).

At 8 weeks, the collagen membranes were completely absorbed, but empty spaces with surrounding inflammatory cells were still observed. In 2 of the 4 specimens, extensive inflammatory cells were distributed around newly formed bone and blank spaces (Figures 4B and 5B).
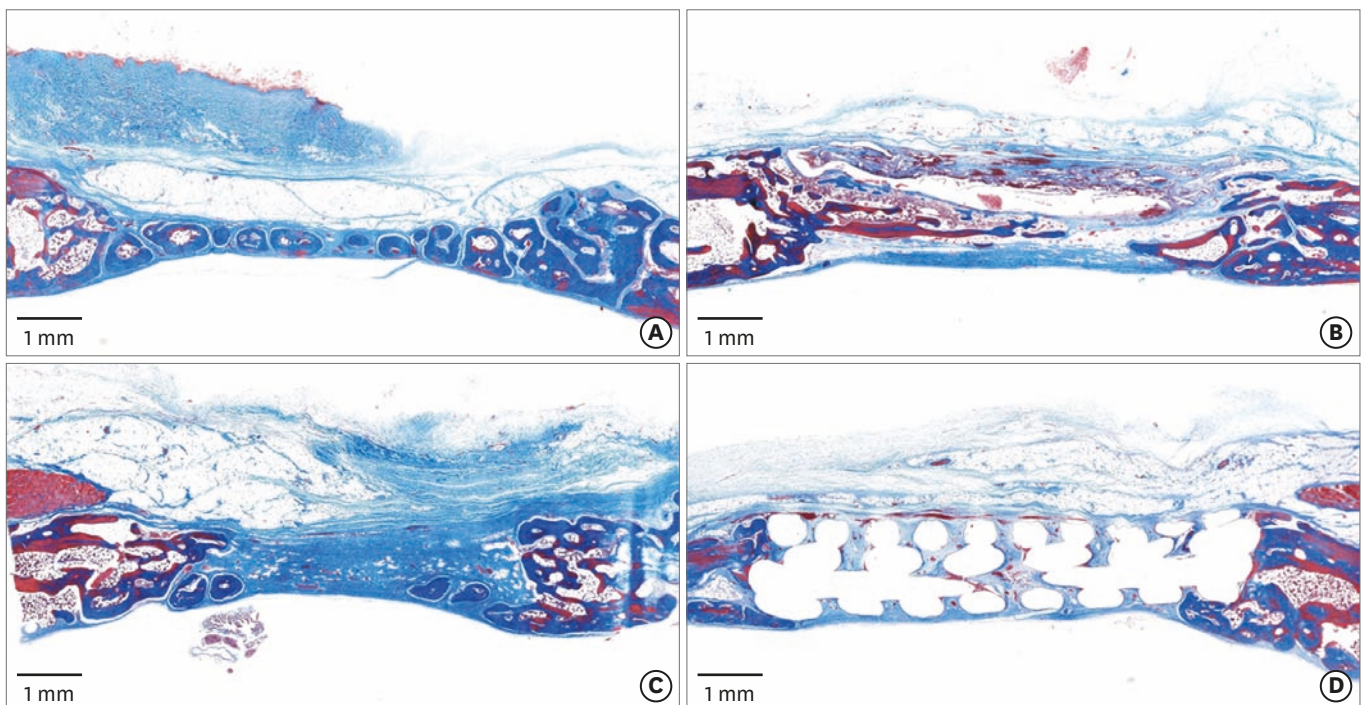
MAP group
At 2 weeks, as in the CA group, the central area surrounded by the membrane and dura mater had collapsed and woven bone structures were seen growing from the peripheral area. The
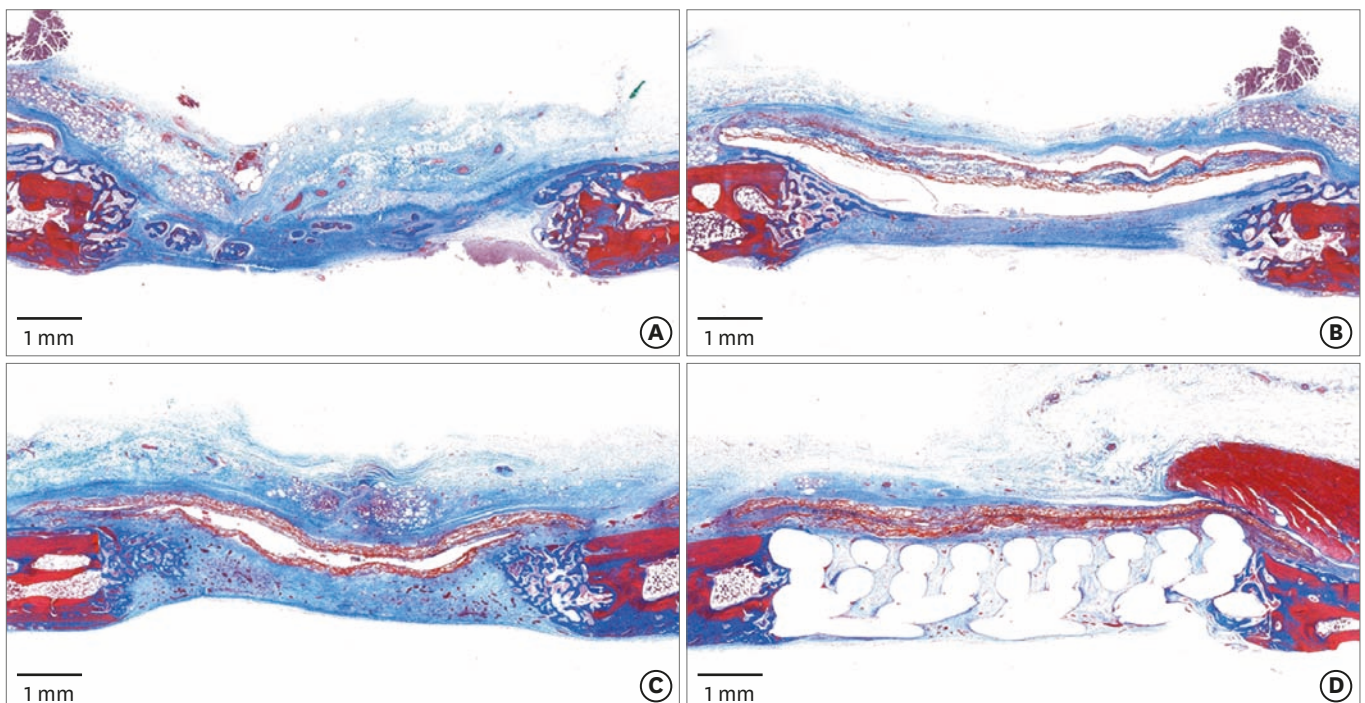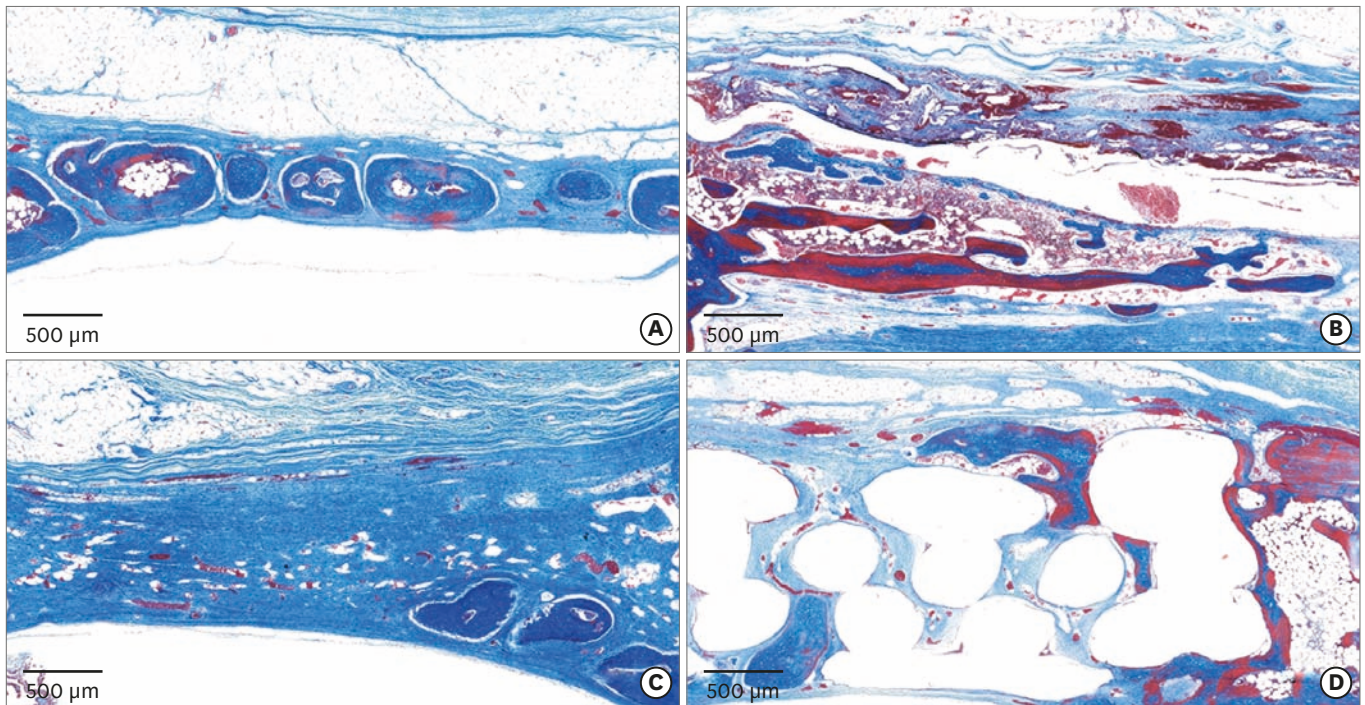

Figure 2. Histologic observations at 2 weeks postoperatively. (A) Control group: the defect had collapsed, but woven bone structures were observed growing from the peripheral area. (B, C) CA and MAP group: the defect was mainly occupied by the connective tissue, and a large space existed below or in the membrane. (D) MAP-PCL group: the defect space was well-maintained by the barrier membrane and supporting PCL block (Masson trichrome staining).
CA: cyanoacrylate, MAP: mussel adhesive protein, MAP-PCL: mussel adhesive protein-polycaprolactone, PCL: polycaprolactone.
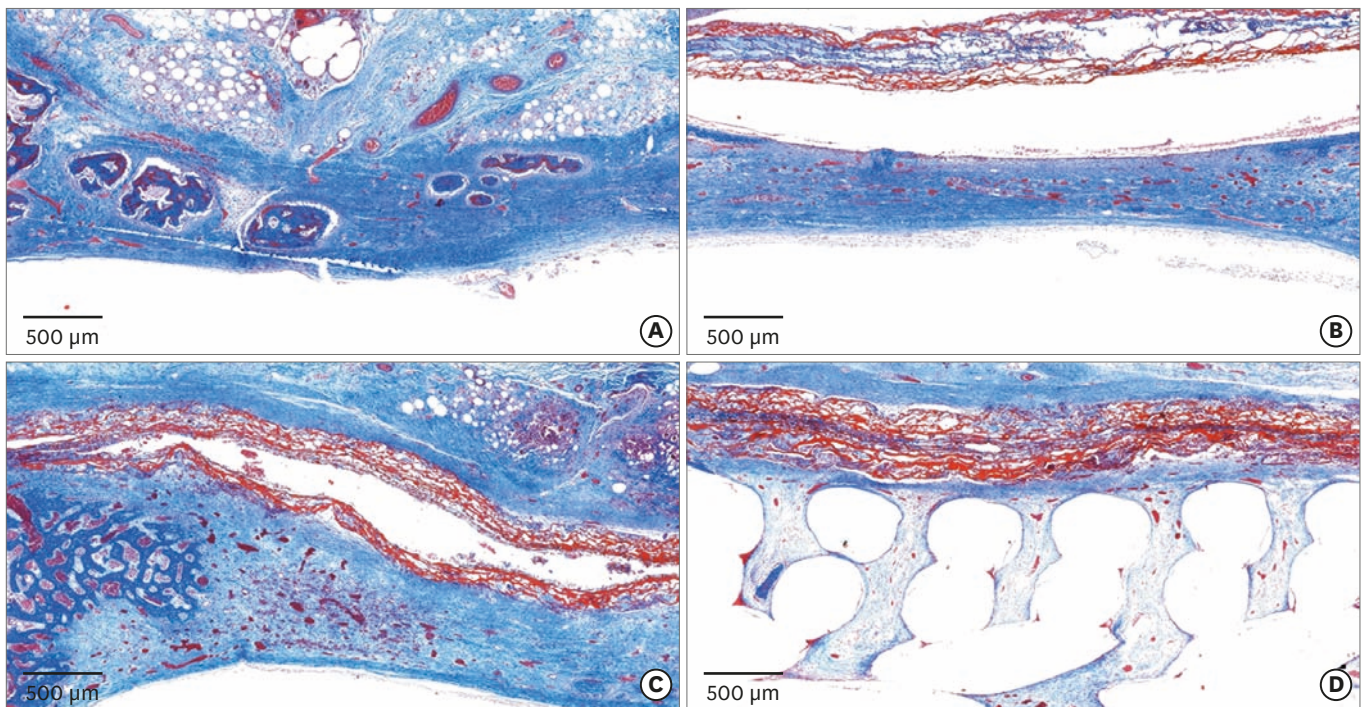
Figure 3. Histologic observations at 2 weeks postoperatively. (A) Control group: a few bony islands were observed. (B, C) CA and MAP groups: the membrane remained present as a collagen network and many newly formed vessels were observed in the defect area. (D) MAP-PCL group: the membrane was closely attached to the block graft and surrounding bone (Masson trichrome staining).
CA: cyanoacrylate, MAP: mussel adhesive protein, MAP-PCL: mussel adhesive protein-polycaprolactone.

Figure 4. Histologic observations at 8 weeks postoperatively. (A) Control group: bone tissue was found in all zones. (B, C) CA and MAP groups: the collagen membranes were no longer observable. In the CA group, blank spaces were still present. (D) MAP-PCL group: the PCL block maintained the original morphology compared to at 2 weeks of healing (Masson trichrome staining).
CA: cyanoacrylate, MAP: mussel adhesive protein, MAP-PCL: mussel adhesive protein-polycaprolactone, PCL: polycaprolactone.

Figure 5. Histologic observations at 8 weeks postoperatively. (A) Control group: formation of bony islands was observed in the central part of the defect. (B) CA group: extensive inflammatory infiltrates were observed around newly formed bone. (C) MAP group: a few bony islands were observed, mainly in the lower part. (D) MAP-PCL group: new bone formation in the upper portion of the block was observed (Masson trichrome staining).
CA: cyanoacrylate, MAP: mussel adhesive protein, MAP-PCL: mussel adhesive protein-polycaprolactone.

barrier membranes remained intact and some specimens exhibited blank spaces around or in the membranes. On a high-magnification view, many blood vessels had infiltrated into the defect area. Additionally, some blood vessels were found within the membrane structure (Figures 2C and 3C).

At 8 weeks, the histologic findings of the MAP and control groups were similar. There were no more residual membranes, and unlike CA group, empty spaces with inflammatory signs were not observed. Formation of bony islands was observed in the central area of the defects (Figures 4C and 5C).

MAP-PCL group
At 2 weeks, new bone had formed from the peripheral area and loose connective tissue was observed in the inner space of the block graft. The membrane was closely attached to the surrounding tissue and block graft. The defect area was well-maintained by the barrier membrane and remaining PCL scaffold. Periosteum-like dense connective tissues were arranged in parallel with the membrane on both the upper and lower sides of the membrane (Figures 2D and 3D).

At 8 weeks, new bone and abundant blood vessels were observed in the inner space of the PCL block. In 1 specimen, new bone had formed between the upper region of PCL and the membrane. Complete degradation of the barrier membrane could be observed, but little degradation of the PCL block had taken place compared to at 2 weeks, and the block stably supported the defect (Figures 4D and 5D).

Table 1. Histometric analysis at 2 and 8 weeks postoperatively

Periods	Group	TA (mm^2)	NB (mm^2)	RG (mm^2)	%NB
2 weeks (n=4)	Control	5.49±1.85[a]	0.88±0.68[b]	-	17.06±11.85
	CA	5.82±2.58[a]	1.60±1.44	-	23.24±13.63
	MAP	5.93±1.90[a]	1.05±0.55[b]	-	16.91±5.74[b]
	MAP-PCL	13.69±1.69	0.76±0.75	7.36±1.02	5.17±4.46
8 weeks (n=4)	Control	7.35±1.29[a]	2.88±1.09[b]	-	39.18±14.83[a]
	CA	6.22±2.46[a]	1.33±1.28	-	18.59±12.37
	MAP	8.09±1.02[a]	2.60±0.65[b]	-	31.77±4.50[a,b]
	MAP-PCL	13.50±0.80	1.82±0.86	6.98±1.49	13.33±5.52

Values are presented as mean±standard deviation.
TA: total augmented area, NB: new bone area, RG: residual graft material area, CA: cyanoacrylate, MAP: mussel adhesive protein, MAP-PCL: mussel adhesive protein-polycaprolactone.
[a]Statistically significant difference from the MAP-PCL group in the same week ($P<0.05$); [b]Statistically significant difference between 2 and 8 weeks in the same experimental group ($P<0.05$).
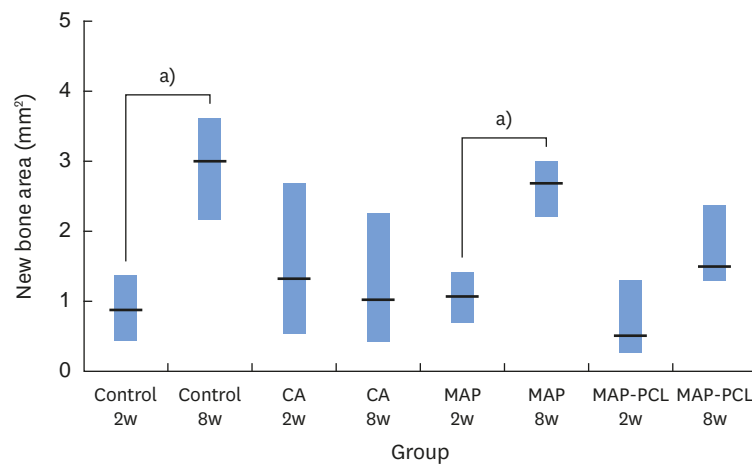
Figure 6. NB in each group.
NB: new bone area, CA: cyanoacrylate, MAP: mussel adhesive protein, MAP-PCL: mussel adhesive protein-polycaprolactone.
[a]Statistically significant difference between groups ($P<0.05$).

Histometric analysis

The results of the histometric analysis results are presented in Table 1. The MAP and control groups showed an increase in the NB between 2 and 8 weeks when compared by period (Figure 6). Furthermore, only the MAP group showed a significant increase in %NB between 2 and 8 weeks. In contrast, the NB in the CA group decreased slightly from 2 to 8 weeks, but the difference was not statistically significant (Figure 6).

In regard to TA, the MAP-PCL group showed greater values than the other groups, which did not have a PCL scaffold throughout the healing period. The RG of the MAP-PCL group between 2 and 8 weeks showed no statistically significant difference. The MAP-PCL group showed a comparable amount of NB to the MAP group.

DISCUSSION

During the GBR procedure, keeping the barrier membrane in place is an important factor for ensuring a predictable result. To ensure the optimal stability of the membrane, various membrane-fixing methods have been developed [2]. Among them, the use of tissue adhesive

in GBR reduces the difficulty of surgery and treatment time [23]. In the present study, MAP exhibited excellent biocompatibility without long-lasting inflammation, and when used with a PCL block, the MAP-loaded collagen membrane seemed to function well as a barrier membrane with good space stability despite its rapid resorption.

In the results of this study, the MAP and CA groups both showed blank spaces around the membranes in most specimens after 2 weeks of healing, implying that adhesive remnants had been present. However, in the histologic analysis of specimens obtained after 8 weeks of healing, MAP exhibited complete absorption, whereas CA remnants were still observed. In the MAP group, there were no byproducts, and the histologic sections showed a similar healing pattern to the control group. It seems that MAP functioned as a fast-degrading and biocompatible adhesive, which may be associated with its ingredients. MAP is composed of various amino acids commonly found in collagen, including tyrosine, the most abundant amino acid in MAP, which plays a key role in adhesion [14,19]. Because none of the amino acids involved in MAP are foreign to vertebrate systems, MAP could be completely absorbed without unwanted byproducts within a short healing period [18-20].

In the present study, CA, which has well-known biocompatible, hemostatic, bacteriostatic, and anti-inflammatory properties, was selected as a positive control adhesive [24-27]. It was reported that CA remained until 90 days, but signs of inflammation were observed only in the early healing periods [3]. However, in this study, 2 out of 4 specimens from the CA group after 8 weeks of healing exhibited extensive inflammatory infiltrates around adhesive remnants. In addition, the histometric analysis of the CA group showed an opposite trend in terms of NB compared with the other groups, even though the difference did not reach statistical significance. The poor results regarding new bone formation seem to have been related to the remnants of the CA adhesives in this study.

The barrier membrane in GBR reduces osteoclastic bone resorption and enhances new bone formation by preventing undesired soft tissue ingrowth into the graft area during the healing period [28-31]. A previous study evaluated the role of the barrier membrane over bone substitutes in the rabbit model, and in the bone graft group, fewer residual particles remained than in the GBR group and fibrous encapsulation of the graft materials in the superficial area was observed [32]. In another experiment, biphasic calcium phosphate block bone substitutes were implanted in rabbit calvarial defects without a barrier membrane. After healing, in the upper part of the block, bone infiltration was minimal and bone regeneration over the block was not visible [33].

In the present study, PCL blocks were implanted in the rabbit calvarial defects and MAP-loaded collagen membranes were used to cover them in the MAP-PCL group. Until 2 weeks of healing, the collagen membranes maintained their collagen network and were closely attached to the block graft and surrounding bone, acting as a barrier against migrating epithelial cells. The same type of collagen membrane was used in a previous study to cover rabbit calvarial defects, and it retained its integrity until 8 weeks [32]. In contrast, in the present study, MAP-loaded collagen membranes were totally absorbed between 2 and 8 weeks, and the result was the same in the CA group. An elevated inflammatory reaction related to the tissue adhesive in the early healing period seems to be an explanation for the difference in the degradation rate between the present and previous studies. It is possible that more extensive inflammatory cell recruitment around adhesives would accelerate the degradation process of the membrane.

Because of fast absorption in the early stage, it is difficult to evaluate the barrier function of the MAP-loaded membrane in the late healing period. However, despite early resorption of the barrier membrane, no soft tissue infiltration from the superior side into the blocks was observed, and new bone was regenerated over the block. In addition, when comparing the NB, a comparable amount of newly formed bone was obtained in the MAP-PCL and MAP groups. In guided tissue regeneration procedures, the first 2 weeks are a critical time for epithelial proliferation [34]. Moreover, the bone and periodontal ligament cells needed for regeneration reach the wound areas within 3–4 weeks [35]. Therefore, the fast resorption rate of the membrane in this experiment seems not to be regarded as a problem, but to obtain more reliable barrier function during the bone regeneration period, it would be proper for the MAP-loaded membrane to have slower degradation rate.

In conclusion, within the limitations of this study, MAP is a biocompatible and biodegradable material usable in GBR procedures. Furthermore, the MAP-loaded membrane functioned efficiently in this rabbit calvarial GBR model. However, the use of tissue adhesives might induce the early degradation of resorbable collagen membranes, and further investigations should attempt to improve the resistance of MAP-loaded membranes against fast resorption. Although the MAP-loaded membrane did not seem to improve bone regeneration compared with the control group, because adhesive facilitates the practical use of membranes, further research may be undertaken to maximize these benefits. In particular, for clinical applications, further studies should assess the effectiveness of MAP in defects with more challenging morphologies than those in the current model.

REFERENCES

1. Retzepi M, Donos N. Guided bone regeneration: biological principle and therapeutic applications. Clin Oral Implants Res 2010;21:567-76.
   PUBMED | CROSSREF

2. Wang HL, Boyapati L. "PASS" principles for predictable bone regeneration. Implant Dent 2006;15:8-17.
   PUBMED | CROSSREF

3. Rezende ML, Consolaro A, Sant'Ana AC, Damante CA, Greghi SL, Passanezi E. Demineralization of the contacting surfaces in autologous onlay bone grafts improves bone formation and bone consolidation. J Periodontol 2014;85:e121-9.
   PUBMED | CROSSREF

4. Pérez M, Fernández I, Márquez D, Bretaña RM. Use of N-butyl-2-cyanoacrylate in oral surgery: biological and clinical evaluation. Artif Organs 2000;24:241-3.
   PUBMED | CROSSREF

5. Choi BH, Kim BY, Huh JY, Lee SH, Zhu SJ, Jung JH, et al. Cyanoacrylate adhesive for closing sinus membrane perforations during sinus lifts. J Craniomaxillofac Surg 2006;34:505-9.
   PUBMED | CROSSREF

6. Rezende ML, Cunha PO, Damante CA, Santana AC, Greghi SL, Zangrando MS. Cyanoacrylate adhesive as an alternative tool for membrane fixation in guided tissue regeneration. J Contemp Dent Pract 2015;16:512-8.
   PUBMED | CROSSREF

7. Baş B, Ozden B, Bekçioğlu B, Sanal KO, Gülbahar MY, Kabak YB. Screw fixation is superior to N-butyl-2-cyanoacrylate in onlay grafting procedure: a histomorphologic study. Int J Oral Maxillofac Surg 2012;41:537-43.
   PUBMED | CROSSREF

8. Chang YY, Dissanayake S, Yun JH, Jung UW, Kim CS, Park KJ, et al. The biological effect of cyanoacrylate-combined calcium phosphate in rabbit calvarial defects. J Periodontal Implant Sci 2011;41:123-30.
   PUBMED | CROSSREF

9. Lu Q, Danner E, Waite JH, Israelachvili JN, Zeng H, Hwang DS. Adhesion of mussel foot proteins to different substrate surfaces. J R Soc Interface 2013;10:20120759.
   PUBMED | CROSSREF

10. Waite JH. Mussel adhesion - essential footwork. J Exp Biol 2017;220:517-30.
PUBMED | CROSSREF

11. Martinez Rodriguez NR, Das S, Kaufman Y, Wei W, Israelachvili JN, Waite JH. Mussel adhesive protein provides cohesive matrix for collagen type-1α. Biomaterials 2015;51:51-7.
PUBMED | CROSSREF

12. Waite JH. Adhesion a la moule. Integr Comp Biol 2002;42:1172-80.
PUBMED | CROSSREF

13. Dove J, Sheridan P. Adhesive protein from mussels: possibilities for dentistry, medicine, and industry. J Am Dent Assoc 1986;112:879.
PUBMED | CROSSREF

14. Castillo JJ, Shanbhag BK, He L. Comparison of natural extraction and recombinant mussel adhesive proteins approaches. In: Puri M, editor. Food bioactives. Basel: Springer; 2017. p.111-35.

15. Yu M, Hwang J, Deming TJ. Role of L-3, 4-dihydroxyphenylalanine in mussel adhesive proteins. J Am Chem Soc 1999;121:5825-6.
CROSSREF

16. Lee H, Scherer NF, Messersmith PB. Single-molecule mechanics of mussel adhesion. Proc Natl Acad Sci U S A 2006;103:12999-3003.
PUBMED | CROSSREF

17. Cha HJ, Hwang DS, Lim S, White JD, Matos-Perez CA, Wilker JJ. Bulk adhesive strength of recombinant hybrid mussel adhesive protein. Biofouling 2009;25:99-107.
PUBMED | CROSSREF

18. Hwang DS, Gim Y, Yoo HJ, Cha HJ. Practical recombinant hybrid mussel bioadhesive fp-151. Biomaterials 2007;28:3560-8.
PUBMED | CROSSREF

19. Grande DA, Pitman MI. The use of adhesives in chondrocyte transplantation surgery. Preliminary studies. Bull Hosp Jt Dis Orthop Inst 1988;48:140-8.
PUBMED

20. Hong JM, Kim BJ, Shim JH, Kang KS, Kim KJ, Rhie JW, et al. Enhancement of bone regeneration through facile surface functionalization of solid freeform fabrication-based three-dimensional scaffolds using mussel adhesive proteins. Acta Biomater 2012;8:2578-86.
PUBMED | CROSSREF

21. Mehdizadeh M, Weng H, Gyawali D, Tang L, Yang J. Injectable citrate-based mussel-inspired tissue bioadhesives with high wet strength for sutureless wound closure. Biomaterials 2012;33:7972-83.
PUBMED | CROSSREF

22. Sohn JY, Park JC, Um YJ, Jung UW, Kim CS, Cho KS, et al. Spontaneous healing capacity of rabbit cranial defects of various sizes. J Periodontal Implant Sci 2010;40:180-7.
PUBMED | CROSSREF

23. Duarte A, Coelho J, Bordado J, Cidade M, Gil M. Surgical adhesives: systematic review of the main types and development forecast. Prog Polym Sci 2012;37:1031-50.
CROSSREF

24. Tseng YC, Hyon SH, Ikada Y. Modification of synthesis and investigation of properties for 2-cyanoacrylates. Biomaterials 1990;11:73-9.
PUBMED | CROSSREF

25. Eiferman RA, Snyder JW. Antibacterial effect of cyanoacrylate glue. Arch Ophthalmol 1983;101:958-60.
PUBMED | CROSSREF

26. Al-Belasy FA, Amer MZ. Hemostatic effect of n-butyl-2-cyanoacrylate (histoacryl) glue in warfarin-treated patients undergoing oral surgery. J Oral Maxillofac Surg 2003;61:1405-9.
PUBMED | CROSSREF

27. Kutcher MJ, Ludlow JB, Samuelson AD, Campbell T, Pusek SN. Evaluation of a bioadhesive device for the management of aphthous ulcers. J Am Dent Assoc 2001;132:368-76.
PUBMED | CROSSREF

28. Dahlin C, Linde A, Gottlow J, Nyman S. Healing of bone defects by guided tissue regeneration. Plast Reconstr Surg 1988;81:672-6.
PUBMED | CROSSREF

29. Weng D, Hürzeler MB, Quiñones CR, Ohlms A, Caffesse RG. Contribution of the periosteum to bone formation in guided bone regeneration. A study in monkeys. Clin Oral Implants Res 2000;11:546-54.
PUBMED | CROSSREF

30. Yang JW, Park HJ, Yoo KH, Chung K, Jung S, Oh HK, et al. A comparison study between periosteum and resorbable collagen membrane on iliac block bone graft resorption in the rabbit calvarium. Head Face Med 2014;10:15.
   PUBMED | **CROSSREF**

31. Jung UW, Lee JS, Lee G, Lee IK, Hwang JW, Kim MS, et al. Role of collagen membrane in lateral onlay grafting with bovine hydroxyapatite incorporated with collagen matrix in dogs. J Periodontal Implant Sci 2013;43:64-71.
   PUBMED | **CROSSREF**

32. Park JY, Jung IH, Kim YK, Lim HC, Lee JS, Jung UW, et al. Guided bone regeneration using 1-ethyl-3-(3-dimethylaminopropyl) carbodiimide (EDC)-cross-linked type-I collagen membrane with biphasic calcium phosphate at rabbit calvarial defects. Biomater Res 2015;19:15.
   PUBMED | **CROSSREF**

33. Lim HC, Song KH, You H, Lee JS, Jung UW, Kim SY, et al. Effectiveness of biphasic calcium phosphate block bone substitutes processed using a modified extrusion method in rabbit calvarial defects. J Periodontal Implant Sci 2015;45:46-55.
   PUBMED | **CROSSREF**

34. Minabe M, Kodama T, Kogou T, Tamura T, Hori T, Watanabe Y, et al. Different cross-linked types of collagen implanted in rat palatal gingiva. J Periodontol 1989;60:35-43.
   PUBMED | **CROSSREF**

35. Iglhaut J, Aukhil I, Simpson DM, Johnston MC, Koch G. Progenitor cell kinetics during guided tissue regeneration in experimental periodontal wounds. J Periodontal Res 1988;23:107-17.
   PUBMED | **CROSSREF**